Nanoscale

Refinements to the Structure of Graphite Oxide: Absolute Quantification of Functional Groups via Selective Labelling

Journal:	*Nanoscale*
Manuscript ID	NR-ART-08-2015-005891.R1
Article Type:	Paper
Date Submitted by the Author:	03-Nov-2015
Complete List of Authors:	Eng, Alex Yong Sheng; Nanyang Technological University, Chua, Chun Kiang; Nanyang Technological University, Chemistry and Biological Chemistry Pumera, Martin; Nanyang Technological University, Chemistry and Biological Chemistry

SCHOLARONE™
Manuscripts

Please do not adjust margins

Nanoscale

FULL PAPER

Refinements to the Structure of Graphite Oxide: Absolute Quantification of Functional Groups via Selective Labelling

Received 00th January 20xx,
Accepted 00th January 20xx

DOI: 10.1039/x0xx00000x

www.rsc.org/

Alex Yong Sheng Eng, Chun Kiang Chua and Martin Pumera*

Chemical modification and functionalization of inherent functional groups within graphite oxide (GO) are an essential aspect of graphene-based nano-materials used in wide-ranging applications. Despite extensive research, there remains some discrepancy in its structure, with current knowledge limited primarily to spectroscopic data from XPS, NMR and vibrational spectroscopies. We report herein an innovative electrochemistry-based approach. Four electroactive labels are chosen to selectively functionalize groups in GO, and quantification of each group is achieved by voltammetric analysis. This allows for the first time quantification of absolute amounts of each group, with a further advantage of distinguishing various carbonyl species: namely *ortho*- and *para*-quinones from aliphatic ketones. Intrinsic variations in the compositions of permanganate versus chlorate-oxidized GOs were thus observed. Principal differences include permanganate-GO exhibiting substantial quinonyl content, in comparison to chlorate-GO with the vast majority of its carbonyls as isolated ketones. The results confirm that carboxylic groups are rare in actuality, and are in fact entirely absent from chlorate-GO. These observations refine and advance our understanding of GO structure by addressing certain disparities in past models resulting from employment of different oxidation routes, with the vital implication that GO production methods cannot be used interchangeably in the manufacture of graphene-based devices.

Introduction

Graphite oxide (GO) is a highly oxidized form of graphite produced through its reaction with various combinations of strong acids and oxidants. Although it was first produced more than 150 years ago,[1] current interest in GO can be much accredited to the initial isolation of graphene[2] and the ensuing fervour to produce large quantities of the material; GO is the key intermediate in the "top-down" approach to producing reduced-graphenes. This seemingly unabating enthusiasm in GO research stems from its uniqueness as a carbon-based material with an assortment of reactive functional groups. Its inherently high specific surface area further enhances its appeal to both materials scientists and synthetic chemists alike as an excellent material on which to perform derivatization or even conversion of specific moieties.[3,4,5] Thus, a plethora of applications exploit these surface groups[6] including bio-functionalization,[7] advanced structural assembly,[8,9] filtration devices,[10] environmental remediation,[11] and electrochemical and biological sensing.[3,12,13] Furthermore, GO's physical properties are tuneable through functionalization,[14,15] and its oxygen groups directly influence its biological toxicity.[16,17]

Despite such widespread utilization of GO, there still remains much debate regarding its complex chemical structure and GO can only be best described as an amorphous material with non-stoichiometric surface functionalities.[18] No less than eight GO structural models have been proposed to date. Chronologically, the earliest model by Hofmann and Holst in 1939 proposed the dominance of epoxides on the basal plane,[19] while Ruess subsequently included hydroxyl groups.[20] Scholz and Boehm[21] then showed the presence of ketones and hydroxyls but excluded epoxides. Much later in 1994, the Nakajima-Matsuo model[22] suggested a lattice structure interspersed with hydroxyl groups. In what is arguably now the most well-known and accepted Lerf-Klinowski model, solid-state nuclear magnetic resonance (NMR) spectroscopy was employed to identify two distinct basal plane regions consisting of pristine aromatic regions separated by aliphatic 6-membered rings containing hydroxyls, epoxyls (1,2-ethers), and C=C double bonds.[23,24] An additional refinement to the model included carboxylic groups in low quantities at the edge sites.[25] Following this, the Dékány model proposed the presence of quinone groups in addition to tertiary alcohols, 1,3-ethers, ketones, and phenols.[26] A later NMR study by Ajayan next included lactols shown to exist at peripheral edges.[27] The latest "Dynamic Structural Model" put forth by Tour in 2013 is also a significant milestone in defining GO as a variable system undergoing structural changes as it interacts

[a] Division of Chemistry & Biological Chemistry, School of Physical and Mathematical Sciences, Nanyang Technological University, Singapore 637371, Singapore. Email: pumera@ntu.edu.sg

Electronic Supplementary Information (ESI) available: Voltammograms of labelled GO at acidic vs. neutral pH; control experiment investigating effects of non-specific adsorption; X-ray photoelectron spectra and Fourier transform infrared spectra of GOs after functionalization and their corresponding controls; Coulombic charges passed from electrochemical redox of labels; detailed calculation of epoxyl content in GO; inherent electrochemistry of GOs; physical images of functionalized and control GOs. See DOI: 10.1039/x0xx00000x

This journal is © The Royal Society of Chemistry 20xx

Please do not adjust margins

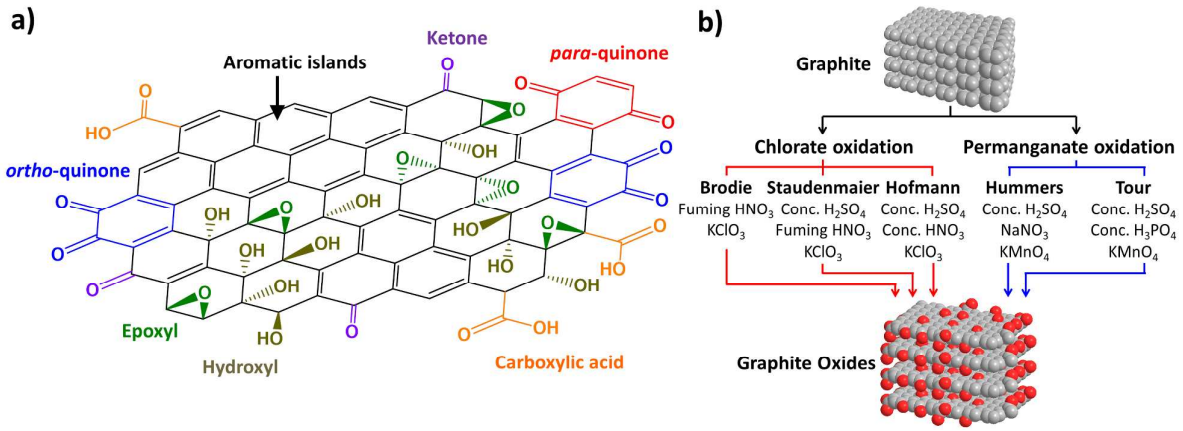

Fig. 1 a) General model of graphite oxide demonstrating various oxygen functional group types distributed across aromatic regions. **b)** Schematic illustration of graphite oxidation methods based either on chlorate or permanganate oxidation routes.

with water, but agrees with earlier models describing the existence of epoxyls, hydroxyls, carbonyls, and carboxyl groups.[28] Fig. 1a depicts a general model of GO summarizing typical oxygen functionalities most commonly proposed.

The variance in structural models is similarly mirrored in the choice of available methods from which GO are produced. All oxidation procedures involve the use of strong concentrated acids with potassium chlorate or permanganate as oxidizing agent (Fig. 1b). Those commonly found in the literature include the pioneering method by Brodie,[1] the Staudenmaier method,[29] and the Hofmann method[30] all utilizing chlorate as oxidant. In comparison, the subsequent methods introduced by Hummers[31] and Tour[32] employ the permanganate route, where the Hummers method is traditionally the most popular due to its short reaction time. Interestingly, close examination of the numerous proposed models reveals that different oxidation methods were used for each study. Thus, it is not unreasonable to question if the choice of oxidation route inevitably led to disparate findings between models. Such a view is not without basis since variations in chemical composition have been determined by techniques such as X-ray photoelectron spectroscopy (XPS) and NMR spectroscopy.[33] Electrochemical measurements further demonstrate unusual reversible behaviour of specific surface functionalities only in permanganate GOs, but not within chlorate GOs.[34-37] Other physical effects also include their dissimilar solvation properties and exfoliation extents depending on oxidation route.[38] Despite this, investigations into the different structures of permanganate and chlorate-oxidized GOs are few and far between, thus with little recognition of this notion within the graphene community.

Towards our objective of identifying the differences in permanganate *versus* chlorate GOs, we employ an established technique previously applied to studying surface functionalities in all manner of carbon materials ranging from pristine graphite, carbon nanotubes and electrodes to their oxidized counterparts, as extensively developed by the groups of Compton and McCreery.[39-47] The two-step approach first involves specific functionalization of different oxygen group types in GO (namely hydroxyls, carboxyls, quinones, carbonyls and epoxyls) with electrochemically active labels, followed by their sensitive voltammetric detection. The nature of voltammetry allows for *absolute* quantification of each labelled group type, and based on the combination of labels chosen the relative content of each functional group is used to quantitatively elucidate the structure of GO. As our current understanding is largely based upon spectroscopic data obtained from XPS, NMR and infrared spectroscopy methods, the application of this electrochemical technique allows for new insights to be observed. One such advancement is the ability to distinguish between different carbonyl functionalities, such as aromatic *ortho*- and *para*-quinones from aliphatic ketones. In this study, we focus our investigation specifically on the Staudenmaier and Hummers GOs due to their prevalence in the literature today,[48] each representing the chlorate and permanganate oxidation routes respectively.

Results and Discussion

A Selective Labelling and Electrochemical Quantification Approach in Studying Graphite Oxide Structures

In this study, we employ electrochemical detection to study the oxygen groups in GO and identify inherent differences in oxygen functionalities present within permanganate-oxidized Hummers GO and the chlorate-oxidized Staudenmaier GO, abbreviated as GO-HU and GO-ST respectively. In four distinct functionalization procedures, oxygen groups are individually reacted with labels either containing an electroactive moiety, or which forms a new electroactive species after reaction. While a stoichiometric excess of each label is used to ensure complete functionalization of all reactive moieties, electrochemical detection of each functional group type is selective since a unique voltammetric signal is only produced with the target group in question.[46] Absolute quantification of each species is

This journal is © The Royal Society of Chemistry 20xx

Please do not adjust margins

Nanoscale

FULL PAPER

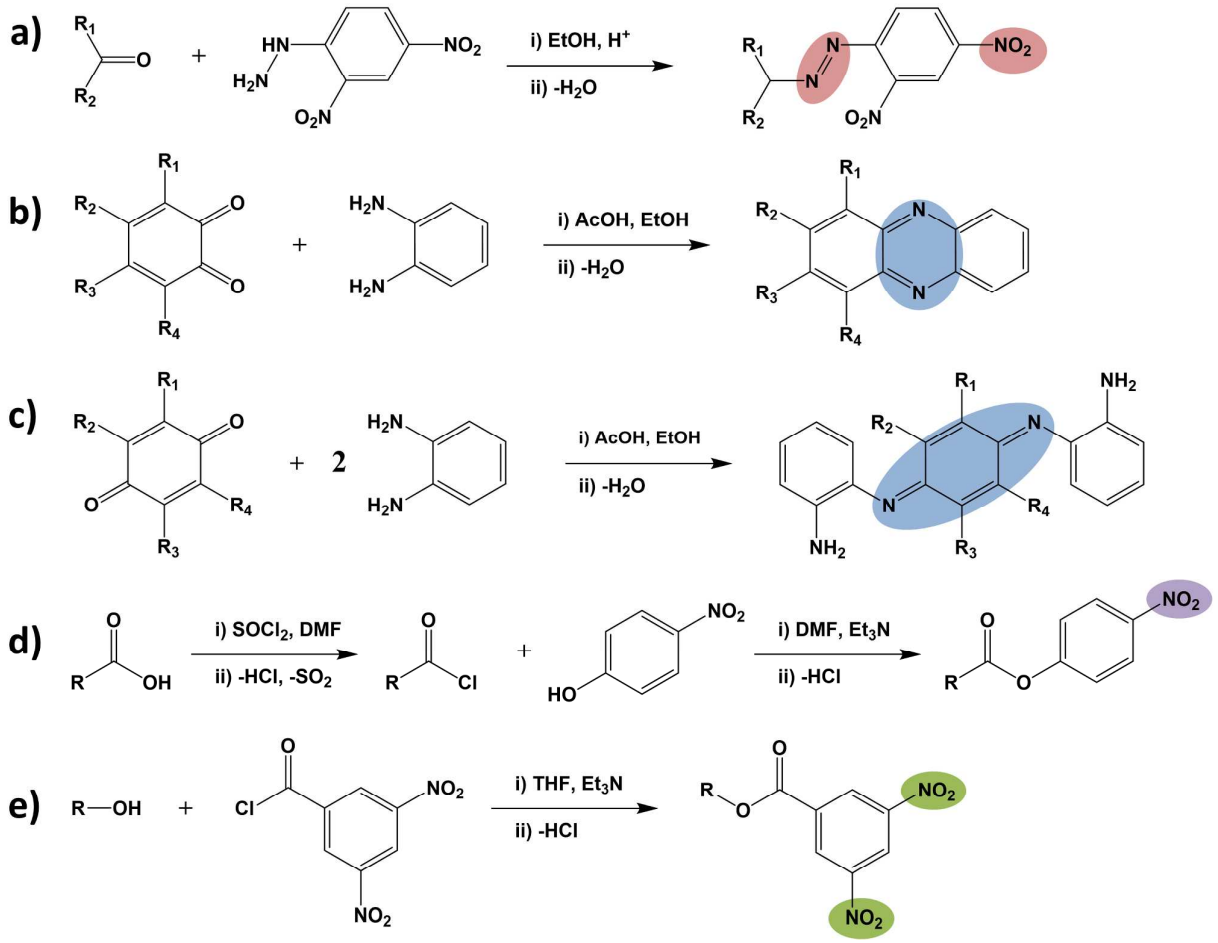

Scheme 1. Selective labelling reactions between functional groups on graphite oxide with electrochemically active labels. Electrochemically active moieties in the final functionalized products are shaded respectively. Labelling of: **a)** carbonyl moieties with 2,4-DNPH to form a new azo-linkage; **b)** *ortho*-quinones with 1,2-PD forming a phenazine adduct; **c)** *para*-quinones with 1,2-PD to give a diimine; **d)** carboxylic acids *via* activation with thionyl chloride and their subsequent esterification with 4-NP; **e)** hydroxyl groups with 3,5-DNBC *via* esterification reaction.

then achieved through voltammetry based on the amount of charge passed during their characteristic electrochemical redox processes. Four reactive labels are chosen that encompass the numerous oxygen group types existing in GO. These reactions are summarized in Scheme 1, with the first reaction between carbonyl groups and 2,4-dinitrophenylhydrazine (2,4-DNPH) to form a new azo-bond with an electroactive nitro moiety. Quinones are further differentiated by selective labelling with 1,2-phenylenediamine (1,2-PD) to give a benzophenazine ring in the case of *ortho*-quinones and a diimine-like adduct when reacted with surface *para*-quinones.[45] Subtraction of quinones from the total carbonyl content thus gives the amount of aliphatic ketones present.[46] Carboxylic groups are first activated with thionyl chloride before the attachment of 4-nitrophenol (4-NP) through esterification. Finally, hydroxyls are labelled using 3,5-dinitrobenzoyl chloride (3,5-DNBC) through condensation with its highly reactive acyl chloride moiety.

Cyclic voltammetry is subsequently performed on both GOs after their individual reaction with one of the four labels. Fig. 2 displays the voltammograms observed for GO-HU after functionalization of its carbonyl, quinonyl, carboxyl and hydroxyl groups respectively. Firstly after functionalization with 2,4-DNPH, the voltammetry of GO-HU shows a characteristically large reduction peak centred near –1.0 V that is not observed in the control GO material. Previous

This journal is © The Royal Society of Chemistry 20xx

Please do not adjust margins

investigations into the reduction mechanism of labelled carbonyls have determined this peak to be from an irreversible $6e^-/6H^+$ process corresponding to the simultaneous reduction of both the azo linkage and the nitro group in the 4-position, followed by cleavage of the entire 2,4-DNPH group leaving behind a nitroso/hydroxylamine moiety.[43] This new surface-bound group is reported to exhibit quasi-reversible electrochemistry between its oxidized and reduced (nitroso/hydroxylamine) states *via* a $2e^-/2H^+$ process centred at approximately –0.1 V *vs* the standard calomel electrode (SCE).[43] An identical redox couple is observed in our case after functionalization with 2,4-DNPH, with its oxidation peak at –0.1 V *vs* Ag/AgCl as illustrated in the Inset of Fig. 2a. In addition, the absence of all voltammetric waves within the control GO confirms that the oxidation peak at –0.1 V occurs only due to labelled carbonyl groups and we therefore use the coulombic charge passed for quantification. The second functional group type studied are quinones which we label with 1,2-PD. As seen in Fig. 2b, two distinct oxidation peaks are observed at –0.5 V and 0.0 V. These peak potentials correspond well to the $2e^-/2H^+$ oxidations of benzophenazine and diimine adducts obtained from the reaction of 1,2-PD with *ortho*-quinones and *para*-quinones respectively (illustrated in Scheme 1b-c).[45] It is most interesting to also note a significant increase in the capacitive current of the 1,2-PD functionalized GO compared to the control GO material, and this was also similarly observed in the earlier case with carbonyl functionalization. Such phenomena are largely expected as a result of extensive functionalization with the labelling molecules,[15,49] likely causing intrinsic changes in the electrical double layer at the GO surface. We subsequently investigate the functionalization of carboxyls with 4-NP but not before their conversion to highly reactive acyl chlorides. Fig. 2c shows the voltammetry of GO-HU after 4-NP labelling, with a familiar oxidation peak at –0.1 V arising from the reversible $2e^-/2H^+$ oxidation of hydroxylamines to nitroso groups.[47] This electrochemistry characteristic of the nitroso/hydroxylamine pair is the same electroactive species that was generated from 2,4-DNPH-labelled GO after cleavage of the azo-linkage. In the present instance with 4-NP-labelled carboxyl groups however, hydroxylamines are instead formed from the nitro moiety in the 4-position during the initial cathodic scan past –0.8 V.[47] Although this conversion of nitro groups to hydroxylamines is not seen as an obvious voltammetric wave, the initial reductive sweep is still important in activating the hydroxylamines which later undergo oxidation to nitroso groups at –0.1 V during the reverse anodic sweep. Additionally, there is a slightly positive shoulder peak at +0.1 V that is also present in the control GO material. Comprehensive controls performed by Compton and co-workers established inherent quinone/hydroquinone systems to be responsible for this peak.[47] Hence, quantification of carboxyl functionalities is based solely on the nitroso/hydroxylamine system at –0.1 V. Finally, hydroxyls were studied through labelling with 3,5-DNBC and their voltammograms displayed in Fig. 2d. A pair of small voltammetric peaks were observed at approximately +0.1 V at the same potentials reported by Jannakoudakis *et al*.[39] This electrochemistry is again based on the nitroso/hydroxylamine system formed from the reduction of nitro groups during the initial cathodic sweep.[39] The slight positive shift in peak potentials is due to the use of an acidic electrolyte at pH 4.0 instead of the neutral pH used for the other materials, and was done to avoid large capacitive background currents that prevented accurate quantification at neutral pH (Fig. S1). At this point, the generally small voltammetric peaks and insignificant changes to the capacitances of GO-HU after its carboxyls and hydroxyls are labelled further support their low contents observed.

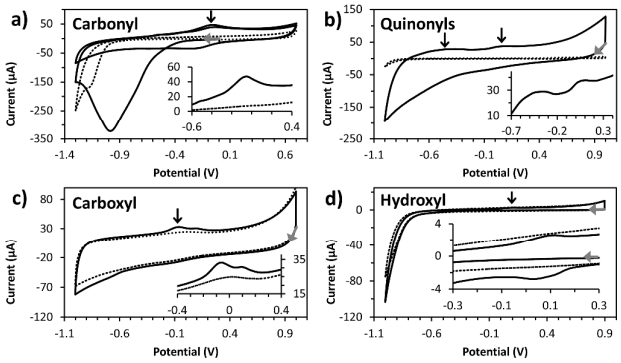

Fig. 2 Cyclic voltammograms of permanganate-oxidized Hummers GO after selective labelling of **a)** inherent carbonyl groups with 2,4-DNPH, **b)** *ortho*- and *para*-quinones with 1,2-PD, **c)** carboxyl groups with 4-NP, and **d)** hydroxyl groups with 3,5-DNBC. Voltammograms of labelled-GOs are shown with solid lines and dotted lines correspond to the control materials. Black open arrows indicate peak oxidations of specific labelled groups as magnified in the Inset figures. Grey arrows indicate the initial starting potentials scanned towards the cathodic direction. Potentials are with respect to the Ag/AgCl reference electrode.

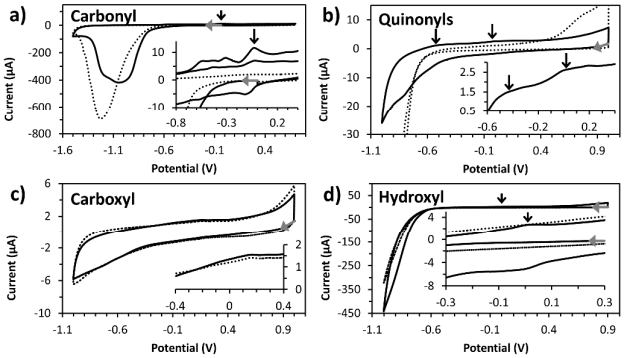

Fig. 3 Cyclic voltammograms of chlorate-oxidized Staudenmaier GO after selective labelling of **a)** inherent carbonyl groups with 2,4-DNPH, **b)** *ortho*- and *para*-quinones with 1,2-PD, **c)** carboxyl groups with 4-NP, and **d)** hydroxyl groups with 3,5-DNBC. Voltammograms of labelled-GOs are shown with solid lines and dotted lines correspond to the control materials. Black open arrows indicate peak oxidations of specific labelled groups as magnified in the Inset figures. Grey arrows indicate the initial starting potentials scanned towards the cathodic direction. Potentials are with respect to the Ag/AgCl reference electrode.

The same experimental labelling and quantification conditions were consequently applied to GO-ST to study its inherent oxygen functionalities. Fig. 3a-d illustrates the voltammograms of GO-ST after functionalization of its carbonyl, quinonyl, carboxyl and hydroxyl groups. First

This journal is © The Royal Society of Chemistry 20xx

examining 2,4-DNPH functionalized GO-ST in Fig. 3a, we observe a contrasting feature in the initial cathodic reduction sweep. Unlike the large reduction peak in functionalized GO-HU that was absent in its control material, the reduction peak of functionalized GO-ST overlapped significantly with the reduction of inherent surface oxygen groups such as epoxides[5052] (as seen in the GO-ST control). This overlap happens because the electro-reduction of GO-ST starts at comparatively lower reductive potentials at *ca*. –0.8 V *vs.* Ag/AgCl, as compared to GO-HU requiring greater cathodic potentials past *ca*. –1.1 V (Fig. S9).[33,34] Such a difference in reduction potentials between GO-ST and GO-HU is typically construed as evidence of their different inherent functional

Table 1. Mole quantities and relative percentages of various functional group types in Hummers graphite oxide (GO-HU) and Staudenmaier graphite oxide (GO-ST) after their functionalization with electroactive labels.

Type of Functional Group	No. of moles measured (mol)		Percentage of total labelled groups (%)	
	GO-HU	GO-ST	GO-HU	GO-ST
Carbonyl (total)	8.0×10^{-10} (± 6%)	6.4×10^{-11} (± 16%)	94.2%	96.3%
• *ortho*-quinone	• 2.6×10^{-10} (± 12%)	• 3.4×10^{-13} (± 58%)	60.4%	1.0%
• *para*-quinone	• 4.6×10^{-11} (± 11%)	• 2.0×10^{-13} (± 20%)	10.8%	0.6%
• Ketone	• 2.0×10^{-10} (± 26%)	• 6.3×10^{-11} (± 16%)	23.0%	94.7%
Carboxyl	4.7×10^{-11} (± 2%)	N.D.	5.5%	0% (N.D.)
Hydroxyl	2.9×10^{-12} (± 35%)	2.4×10^{-12} (± 12%)	0.3%	3.7%
Total labelled groups	8.5×10^{-10} (± 6%)	6.6×10^{-11} (± 15%)	100%	100%

Notes: Calculations of absolute functional group contents are based on the coulombic charges passed during electrochemical oxidation of each label. GO mass per electrode = 2.0 µg. *n* = 3, absolute mole quantities rounded to two significant figures. N.D. denotes "not detected".

group types. Other features in 2,4-DNPH-labelled GO-ST absent in GO-HU are the small oxidative waves observed between –0.6 V to –0.35 V. Since these are not observed in the control GO-ST, we postulate that they must arise from interactions of the 2,4-DNPH label and specific groups in GO-ST not found in GO-HU. In spite of these, quantification of labelled carbonyl groups in GO-ST is nevertheless possible based on the same nitroso/hydroxylamine system at –0.1 V. Next, the voltammetry of 1,2-PD-labelled GO-ST (Fig. 3b) is largely analogous to the GO-HU case, albeit with discernibly smaller oxidation peak currents from *ortho*- and *para*-quinones at –0.4 V and 0.0 V along with a greatly reduced capacitive background current. This result signifies the relatively lower quinonyl composition in GO-ST. The most interesting observation however is for 4-NP-reacted GO-ST in Fig. 3c, where the voltammograms of both the reacted material and its control were virtually indistinguishable, thus indicating a total absence of carboxyls in GO-ST. We similarly noted this finding based on solid-state ^{13}C NMR spectroscopy previously.[33] Lastly, the oxidation peak of the nitroso/hydroxylamine system is seen at 0.0 V (Fig. 3d) for 3,5-DNBC-labelled GO-ST with similar current intensities as GO-HU.

As this is the first instance that the above labelling and voltammetric quantification approach has been applied to the study of GO functional groups and their structures, we deem it prudent to emphasize the fundamental requirements for quantifying the functionalities in GO. These include *(1)* attaining complete functionalization of all groups in GO with the labelling molecules used, and also *(2)* the absence of non-covalent attachment (*eg*. physical adsorption) of electroactive labels that would otherwise result in an overestimate of the amount of functional groups. Nevertheless, steps can be taken to effectively mitigate these. The first requirement is easily addressed by utilizing reactions involving highly reactive moieties that typically attain near 100% reaction yields. One such example is the activation of carboxylic groups to the acyl chloride before covalent attachment with 4-NP, in consideration of the weakened nucleophilicity of 4-NP conferred by the nitro group. Thus, the final amounts measured would provide for a realistic elucidation of actual GO structures. We also confirmed that there are no contributing effects from non-specific adsorption of the nitroaromatic labels used, by performing additional control reactions with GO and nitrobenzene. Specifically, the characteristic voltammetric waves of the nitro moiety were absent and no changes were observed in the inherent electrochemistry of GO-HU (Fig. S2). This was further corroborated with XPS showing neither a new nitrogen peak nor any change in the high resolution C 1s spectra. Hence, it is shown that selective functionalization of oxygen-containing groups in GO allows for their reliable detection through absolute quantification of the covalently attached electroactive labels.

Comparison of Functional Groups in Graphite Oxides Produced From Permanganate *versus* Chlorate Oxidation Methods and Their Correlation to Proposed Models

Consequently based on the observed voltammetry of the various electroactive labels, the amount of each surface functional group in GO is calculated by use of Faraday's Law of Electrolysis.[34,45,47,50] Table 1 summarizes the quantification data of the various functionalities in GO-HU and GO-ST after their labelling. The amounts of some functionalities present are found to be strikingly different for the permanganate-oxidized GO-HU in comparison to GO-ST from the chlorate route. In terms of absolute mole quantities, the total average

labelled-group content detected in GO-HU (8.5×10^{-10} mol) is one order of magnitude larger than in GO-ST (6.6×10^{-11} mol). Within both GOs, carbonyls were also seen to represent the vast majority of surface groups at ~95%. However, our use of 1,2-PD labelling further discerns quinones from isolated ketones, where the amount of ketones can be acquired by direct subtraction of quinones from the total carbonyl content (and that each quinone contains two C=O groups). We observed for the case of GO-HU that *ortho*-quinones constitute more than 60% of all labelled oxygen groups, followed by isolated ketones at 23% and *para*-quinones at just about 11%. This distribution is however very different with GO-ST where isolated ketone groups were deduced to be dominant at nearly 95%, compared to insignificant amounts of quinones at ≤1% for each form. The small absolute quantity of *ortho*-quinones particularly in GO-ST is also likely to have resulted in its high percentage error. Nonetheless *ortho*-quinones were found to be more abundant than *para*-quinones in both GOs, and since carbonyls have been shown to mainly decorate sheet edges,[54] we reason that *para*-quinones simply cannot exist in sizable amounts because its 1,4-geometry would structurally limit the size of GO sheets. Such abundance of quinones in GO-HU, as opposed to its scarcity in GO-ST, is in line with our earlier proposition that quinone/hydroquinone couples are likely responsible for the unusual reversible electrochemistry observed only in permanganate-oxidized GOs.[34,36] Subsequent computation of the carboxyl content shows that it contributes only a low 5.5% in GO-HU and is entirely absent in GO-ST. Finally, examination of hydroxyls reveals comparable amounts at between 2.4×10^{-12} mol and 2.9×10^{-12} mol for GO-HU and GO-ST. These values constitute surprisingly low quantities relative to the overall oxygen group content at only 3.7% for GO-ST and a mere 0.3% for GO-HU, in disagreement with many proposed models citing hydroxyls as amongst the most prevalent species.[20-28] Since hydroxyls tend to cluster together in highly oxidized regions,[53,54] it may be possible that steric effects could hinder functionalization of the label onto some closely assembled hydroxyl groups and the amount detected might therefore represent a lower bound of the actual value. This is likely to have also resulted in the amount of hydroxyls having the largest percentage error of all functional groups in GO-HU.

We then correlate these results with materials characterization data providing chemical compositions and bonding information to confirm the functionalization of labels. As XPS is a surface sensitive technique well suited to studying surface functionalization of carbon materials,[55] one measure of successful labelling is the carbon-to-oxygen ratio (C/O ratio) where a lower value corresponds to a greater distribution of surface oxygen groups. Wide-scan XPS spectra of all functionalized and control GO-HU materials are displayed in Fig. S3 of the Supplementary Information, with their elemental compositions documented in Tables S1 and S2. C/O ratios of the parent GO-HU and GO-ST are typically low at 2.12 and 2.48 indicating high surface oxygen contents. Consequently from the high extents of functionalization of carbonyls and quinonyls, C/O ratios more than double due to the loss of oxygen as a result of the condensation reactions (Scheme 1a-c), thus corroborating with voltammetry results. Moreover, the C/O ratios of the control materials remained low with negligible change, proving that experimental conditions did not intrinsically alter the GO. These findings concur with high resolution carbon 1s spectra (Fig. S4 and S5) showing decreases in C–O and C=O groups after labelling; again no changes were observed between the controls and the parent GOs.[33] Most importantly however, a benefit of employing nitrogenous labels is the introduction of new nitrogen 1s signals that permit assessment of the functionalization.[45,46,47] Both 2,4-DNPH-labelled GO-HU and GO-ST show two peaks at 400 eV from the azo-linkage and at 406 eV from nitro groups (Fig. S6), whereas the reaction of 1,2-PD with *ortho*- and *para*-quinones gives characteristic peaks at about 398.5 eV and 399.5 eV respectively from pyrazine and arylamine adducts.[56,57] With 4-NP and 3,5-DNBC-labelled GO however, only minor differences in XPS were observed in relation to their controls. The use of thionyl chloride in the activation of carboxyls inevitably led to its reaction with other moieties like hydroxyls and epoxyls which resulted in their removal. Negligible changes in C/O ratios and the C 1s spectra of GOs were seen after hydroxyl labelling, in agreement with their small amounts as we detected. Despite this, minute peaks from the nitro moiety of the 3,5-DNBC label were nonetheless discernible in their N 1s spectra. In comparison, we find that FTIR spectroscopy holds minimal diagnostic ability due to its lack of surface sensitivity, but more so because the opaque nature of GO frequently results in poor quality spectra (Fig. S7-S8).[46] This is further complicated with the overlap of many important stretches arising from both surface groups themselves and the labelling molecules, such as inherent C=C stretches[26,33] from the sp^2 carbon lattice with azo (–N=N–) and imino (–C=N–) moieties[58] from GO adducts all occurring within the same 1690–1575 cm^{-1} region. Hence, chemical information from XPS but not FTIR can be effectively used to track the labelling process and thus validates the results from the electrochemical labelling and detection of functional groups in GO.

Thus far, we have yet to acquire inherent epoxyl concentrations despite its known prevalence in GO.[23-28,33,53,54,59] However, the information garnered from the four labels chosen for this study allows us to deduce the epoxyl quantity present in GO-HU. Of the four labels, only 2,4-DNPH and 1,2-PD contain amine moieties, which as strong nucleophiles are commonly used to attack epoxide groups in GO.[60-63] Our XPS data supports this conclusion due to the loss of C-O bonding modes in GO after both reactions. While the reaction between 1,2-PD and epoxyls does proceed to give secondary amines, these adducts are electrochemically inactive. 4-NP in comparison is a much weaker nucleophile, and more importantly the prior use of thionyl chloride deactivates hydroxyls and epoxyls (as observed from XPS), therefore preventing any complication should epoxyl functionalization occur. Hence, only the 2,4-DNPH label

This journal is © The Royal Society of Chemistry 20xx

maintains electroactive nitro moieties from which to quantify labelled epoxides. As discussed in the previous section, the electrochemical redox mechanism of 2,4-DNPH labels involves an initial $6e^-/6H^+$ reduction at –1.0 V due to a $2e^-/2H^+$ reduction of the azo-linkage occurring simultaneously with a $4e^-/4H^+$ reduction of nitro groups at the 4-position.[43] Assuming this similar mechanism for labelled epoxyls, we can then deduce the epoxyl amount through subtraction of the labelled carbonyls with their oxidation occurring at –0.1 V (detailed calculation is shown in the Supplementary Information).

Table 2. Relative abundances of various functional groups in Hummers graphite oxide (GO-HU).

Type of Functional Group	Percentage of total labelled groups (%)
Epoxyl[a]	75.4%
Carbonyl (total)	23.2%
• *ortho*-quinone	• 14.9%
• *para*-quinone	• 2.6%
• Ketone	• 5.7%
Carboxyl	1.3%
Hydroxyl	0.1%

Note: Percentages are calculated based on voltammetric quantification. [a] The epoxyl content is deduced based on its reaction with 2,4-DNPH, with assumption of the $6e^-/6H^+$ reduction mechanism from Ref 43.

The average epoxyl content for GO-HU is therefore determined at 2.6×10^{-9} mol. This is re-calculated with all functionalities to give the relative abundance of oxygen groups in GO-HU, as tabulated in Table 2. Regrettably, the above derivation of epoxyl moieties is only possible for GO-HU and not for GO-ST due to a large overlap of its inherent reduction with that of the 2,4-DNPH label as illustrated in Fig. 3a.[33,34]

Therefore, a summary of the functionalities in GO-HU detected through the electrochemical labelling approach is as such: *(1)* epoxyls are most abundant in GO at approximately three-quarters of all functionalities; *(2)* carbonyls account for slightly less than a quarter of all groups, of which *ortho*-quinones represent the majority followed by aliphatic ketones and finally *para*-quinones; *(3)* carboxyls exist at only 1.3% despite the traditionally held view that they contribute to the inherent acidity of GO;[64] and also that *(4)* the amount of labelled hydroxyls is unexpectedly small. In assessing the significance of the quantification data with respect to current GO models, we first examine the dominance of epoxyl groups in GO, which is largely accepted based on NMR evidence.[23-28,33,59] They are known to be dispersed throughout the basal plane,[53,54] and exhibit high reactivities to nucleophiles such as amines.[60,62] In contrast, hydroxyls can congregate in densely oxidized regions[53] and we cannot exclude the possibility of a small contribution from steric effects which lead to the low proportion of hydroxyls detected from labelling. Two *in situ* processes would however pose a greater influence that likely resulted in the relatively small amount of hydroxyl groups measured: Klinowski and co-workers first acknowledged the instability of C–OH groups that condense to form C–O–C (ether or epoxide) linkages,[23] while Tour further expounded upon a possible disproportionation of C–OH bonds to give C=C and C=O bonds.[28] It is thus conceivable that some hydroxyls have disproportionated as such to give the significantly high amounts of both epoxyl and quinone groups detected. Additionally, an interesting association between carbonyls and hydroxyls was also found with most existing in the form of vinylogous acids,[28] accounting for the inherent acidity of GO which cannot arise from such small concentrations of carboxylic groups at *ca*. 1% measured for GO-HU. Predominant only at the sheet edges,[65] they are unlikely to even be present in considerable amounts. Moreover, this acidity is characteristic in all GOs, including chlorate-oxidized GO-ST where we found a total absence of carboxylic groups. Our results strongly suggest that only the permanganate oxidation methods produce carboxyl functionalities, however little may be present. In further support of our proposition, only the models by Lerf-Klinowski[25] and Tour[28] found any presence of carboxyls while the Ajayan model[27] included a minute contribution from lactols as a carboxyl derivative; it is interesting to note that these models studied permanganate-oxidized GOs exclusively. We contrast this to earlier models[19-22] and also the Dékány model[26] primarily employing chlorate oxidations with the effect that no obvious evidence for carboxyls were found. Hence, while the relative percentages of groups generally agree well with current proposed models, we also note that GO is intrinsically variable due to functional group conversions. The use of this selective labelling approach coupled with electrochemistry detection has thus given much insight into dissimilar GO structures obtained through different oxidation routes.

Conclusions

In this study, an electrochemical detection approach was applied towards investigating the structure of graphite oxide through functionalization of its various oxygen groups, providing a new perspective from current knowledge predominantly based upon spectroscopic techniques. This selective labelling method is established within the study of surface functionalities for a diverse selection of carbon materials, but is as yet unexploited for any graphene-type material. Four reactive labels containing electrochemically active moieties were chosen to individually target carbonyl, quinonyl, carboxyl, and hydroxyl groups in GO, allowing for their quantitative information to be obtained *via* voltammetric analysis. The results interestingly reveal major differences in functional group distributions within permanganate-oxidized (Hummers) GO *versus* chlorate-oxidized (Staudenmaier) GO. The selectivity also enables us for the first time to distinguish the different types of carbonyl species present in GO, namely *ortho*- and *para*-quinones from aliphatic ketones. Hummers GO was found to have a substantial amount of *ortho*-quinones as compared to Staudenmaier GO with aliphatic ketones

forming the vast majority of its carbonyl content. More notably, only a small amount of carboxyls were found (in Hummers GO) consistent with latest reports, and are furthermore absent entirely from Staudenmaier GO. As is expected from proposed models, we similarly deduced that epoxides are the predominant species within Hummers GO. The hydroxyl contents observed after labelling are also generally low, suggesting the occurrence of proposed disproportionation reactions that result in the formation of other groups. In light of these observations, we wish to reiterate on the importance of the choice of oxidation routes in the manufacture and application of GO materials since variations in their structure can radically influence intended results. Although minor limitations currently exist (particularly in the analysis of epoxides present in Staudenmaier GO), their absolute quantification may be achieved in future with the use of orthogonal labels specifically targeting epoxyls. Nevertheless, this approach has provided new information towards a better overall understanding of GO structures.

Experimental

Materials

Graphite (<20 mm), sulfuric acid (95–98%), sodium nitrate, hydrochloric acid (37%), phosphoric acid (85%), potassium chlorate (98%), N,N-dimethylformamide (DMF), tetrahydrofuran (THF), ethanol (EtOH), diethyl ether, hydrogen peroxide (30%), 2,4-dinitrophenylhydrazine (2,4-DNPH) in phosphoric acid, potassium phosphate dibasic, and sodium phosphate monobasic were purchased from Sigma–Aldrich (Singapore). 1,2-phenylenediamine (1,2-PD), 3,5-dinitrobenzoyl chloride (3,5-DNBC), 4-nitrophenol (4-NP) were obtained from Alfa Aesar. Potassium permanganate and fuming nitric acid (>90%) were obtained from J.T. Baker. Glassy carbon (GC) electrodes with a diameter of 3 mm and a platinum auxiliary electrode were obtained from CH Instruments (USA). Milli-Q water (resistivity: 18.2 MΩ cm) was used throughout the experiments. Electrochemical measurements were done in a 5 mL electrochemical cell with a three-electrode configuration using an Autolab PGSTAT 101 electrochemical analyzer (Eco Chemie, Utrecht, The Netherlands). All electrochemical potentials are reported relative to the Ag/AgCl reference electrode.

Procedures

GO preparation via the modified Hummers Method.[31] 0.5 g of graphite was initially added to sulfuric acid (23.0 mL, 95–98%) with stirring for 20 min at 0 ^{o}C, followed by the addition of 0.5 g $NaNO_3$ portion-wise and stirred for 1 h. With the temperature kept at 0 ^{o}C, $KMnO_4$ (3 g) was subsequently added slowly, and the mixture then heated to 35 ^{o}C for 1 h. 40 mL of water was then added into the mixture, and consequently resulted in the temperature rising to ~90 ^{o}C and further maintained for 30 min. An additional 100 mL of water was added, followed by the slow addition of approximately 10 mL H_2O_2 (30%). The warm solution was filtered through an RC membrane (0.22 μm) and washed with warm water (100 mL). The solid was finally washed with a copious amount of water until a neutral pH was obtained and kept in the oven at 50 ^{o}C for five days before experimental use.

GO preparation via the Staudenmaier Method.[29] Concentration sulfuric (17.5 mL, 95–98%) and nitric acids (9 mL, >90%) were first added to a reaction flask, and stirred at 0 ^{o}C for 15 min. 1 g of graphite was then added to the mixture and stirred vigorous to obtain a homogeneous dispersion. Potassium chlorate (11 g) was subsequently added in portions to the mixture slowly over 15 min, to avoid sudden increases in temperature and rapid formation of chlorine dioxide (Caution: ClO_2 gas is explosive at high concentrations). With complete dissolution of potassium chlorate, the reaction flask was loosely capped to allow evolution of gas, and stirring was continued vigorously at room temperature for 96 h. The resulting slurry was then poured into ultrapure water (1 L), filtered, then re-dispersed and washed repeatedly in HCl solutions (5%) to remove sulfate ions. The GO was lastly washed with ultrapure water until a neutral pH of the filtrate was obtained. The GO slurry was then dried in a vacuum oven at 50 ^{o}C for five days before use.

2,4-Dinitrophenylhydrazine(2,4-DNPH) Functionalization of Carbonyl Groups.[43,44] Each GO (20 mg) was ultrasonicated in EtOH (20 mL, 1 mg mL^{-1}) for 1 h. Excess 2,4-DNPH (5.4 mL, 0.2 M) in phosphoric acid was added to the GO suspension, and the same volume of phosphoric acid (85%) was added to the control mixture. The mixture was stirred for 20 h at 80 ^{o}C under reflux. The GO was obtained by vacuum filtration and sequentially washed with EtOH, water and ether until a more neutral pH (5-6) was obtained. The functionalized material was then dried in under vacuum at 30 ^{o}C for 48 hours before analysis.

1,2-Phenylenediamine (1,2-PD) Functionalization of Quinonyl Groups.[45,46] GOs (20 mg) were first ultrasonicated for 1 h in glacial acetic acid at 1 mg mL^{-1} concentration. 1,2-PD (77 mg) was separately dissolved in EtOH (2 mL) and then added to the GO suspension; only pure EtOH was added to the control mixture. The mixture was then stirred for 1 h at 95 ^{o}C. The reacted GO was obtained by vacuum filtration and washed with EtOH, water and ether. The pH of the filtrate increased with each wash giving a final stable value *ca*. pH 6. The reacted GO was finally dried in vacuum oven at 30 ^{o}C for 48 hours before experimental usage.

4-Nitrophenol (4-NP) Functionalization of Carboxylic Groups.[46,47] The first step involves conversion of carboxylic groups to the highly reactive acid chloride moiety as modified from previous procedures.[66,67] Each GO (60 mg) was ultrasonicated for 1 h in pure DMF at 1 mg mL^{-1} concentration. $SOCl_2$ (1 mL, 0.014 mol) was added dropwise and the mixture stirred at r. t. for 20 h. The reaction was carried out with a Schlenk line under N_2 atmosphere. Excess $SOCl_2$ was subsequently removed by heating to ~80 ^{o}C with the reaction

 This journal is © The Royal Society of Chemistry 20xx

flask fitted with a $CaCl_2$ guard tube. This acyl chloride-converted GO mixture was split into two 30 mL portions. Under N_2 atmosphere, 4-NP (960 mg) was dissolved in DMF (5 mL) and added to the reaction mixture, and only pure DMF added to the control. Triethylamine (2 mL) was added dropwise to each mixture (Note: small amounts of white triethylamine hydrochloride salt forms upon initial addition). Both mixtures were stirred for 20 h and the final functionalised GO obtained by vacuum filtration and washed with large amounts of DMF, followed by water and ether. The product was lastly dried in a vacuum oven at 30 ^{o}C for 48 hours before use.

3,5-Dinitrobenzoyl Chloride (3,5-DNBC) Functionalization of Hydroxyl Groups.[39,40,41,42] Each GO (20 mg) was ultrasonicated for 1 h in THF at a concentration of 1 mg mL^{-1}. 3,5-DNBC (165 mg) was separately dissolved in THF (1.5 mL) and added to the GO suspension slowly under stirring, while only pure THF was added to the control mixture. 2 mL of triethylamine was added dropwise subsequently and the mixture was stirred for 20 h at room temperature. The functionalized GO was obtained by vacuum filtration and washed with copious amounts of THF, followed by deionised water and ether. The final product was lastly dried in a vacuum oven at 30 ^{o}C for 48 hours before use.

Voltammetric Quantification of Labelled Functional Groups
Functionalized graphene oxides and their control materials were first dispersed in DMF at 1 mg mL^{-1} concentrations by ultrasonication for 10 min to obtain stable graphene oxide suspensions, while a 5 min sonication was performed before each electrode modification step. GC working electrodes were cleaned and renewed just prior to every measurement by polishing with a 0.05 µm alumina particle slurry on a polishing pad and followed by copious washing with deionized water. 1.0 µL aliquots were deposited onto the GC electrode surface, and the solvent left to evaporate at room temperature. This process was performed twice to achieve a uniform coating, thus giving a fixed sample mass of 2.0 µg immobilized per electrode each with a geometric surface area of 0.0707 cm^2. Electrochemical measurements were performed in 50 mM phosphate-buffered saline (PBS) solution as supporting electrolyte, with the buffer providing a constant supply of protons required for the electrochemical redox of labelled groups. A neutral pH 7.2 was used in the detection of all functionalized oxygen groups with the exception of labelled hydroxyls which required an acidic pH of 4.0. A fixed scan rate of 100 mV s^{-1} was used in all cyclic voltammetry experiments other than a slower 50 mV s^{-1} employed specifically for labelled carbonyls to allow for full development of its broad reduction peak centered at –1.0 V. Absolute quantification of labelled surface groups is based on Faraday's Law of electrolysis:[34,45,47,50]

$$n = \frac{Q}{z \times F} \qquad \text{(Equation 1)}$$

where n is the number of moles of surface-bound species undergoing an electrochemical redox reaction, Q is the total charge passed, *z* is the number of electrons exchanged per surface group, and F is the Faraday constant (96485 C mol^{-1}). For consistency, calculations are based on the charges passed within the oxidation peak occurring during the initial anodic scan. Functional group contents are calculated based on the average from triplicate measurements.

Materials Characterization
XPS was done using a Phoibos 100 spectrometer with an Mg Kα X-ray radiation source (SPECS, Germany) for the measurement of wide-scan survey spectra and high-resolution C 1s and N 1s spectra. Relative sensitivity factors were used for evaluating C/O ratios. GO samples were prepared by compacting a layer of the materials onto conductive carbon tape. FTIR spectra of GO samples were obtained from a PerkinElmer 100 system fitted with a universal attenuated total reflectance (ATR) accessory with a Diamond/ZnSe crystal.

Acknowledgements

M.P. acknowledges Tier 2 grant from the Ministry of Education, Singapore.

Notes and references

1 B. C. Brodie, *Philos. Trans. R. Soc. London*, 1859, **149**, 249–259.
2 K. S. Novoselov, A. K. Geim, S. V. Morozov, D. Jiang, Y. Zhang, S. V. Dubonos, I. V. Grigorieva and A. A. Firsov, *Science*, 2004, **306**, 666–669 .
3 D. Chen, H. Feng and J. Li, *Chem. Rev.*, 2012, **112**, 6027–6053.
4 C. K. Chua and M. Pumera, *Chem. Soc. Rev.*, 2013, **42**, 3222–3233.
5 V. Georgakilas, M. Otyepka, A. B. Bourlinos, V. Chandra, N. Kim, K. C. Kemp, P. Hobza, R. Zboril and K. S. Kim, *Chem. Rev.*, 2012, **112**, 6156–6214.
6 Y. Zhu, D. K. James and J. M. Tour, *Adv. Mater.*, 2012, **24**, 4924–4955.
7 Y. Wang, Z. Li, J. Wang, J. Li and Y. Lin, *Trends Biotechnol.*, 2011, **29**, 205–212.
8 I. P. Hamilton, B. Li, X. Yan and L. Li, *Nano Lett.*, 2011, **11**, 1524–1529.
9 S. R. Shin, B. Aghaei-Ghareh-Bolagh, X. Gao, M. Nikkhah, S. M. Jung, A. Dolatshahi-Pirouz, S. B. Kim, S. M. Kim, M. R. Dokmeci, X. Tang and A. Khademhosseini, *Adv. Funct. Mater.*, 2014, **24**, 6136–6144.
10 D. V. Kosynkin, G. Ceriotti, K. C. Wilson, J. R. Lomeda, J. T. Scorsone, A. D. Patel, J. E. Friedheim and J. M. Tour, *ACS Appl. Mater. Interfaces*, 2012, **4**, 222–227.
11 J. G. S. Moo, B. Khezri, R. D. Webster and M. Pumera, *ChemPhysChem*, 2014, **15**, 2922–2929.
12 Y. Zhang, M. Qi and G. Liu, *Electroanal.*, 2015, **27**, 1110–1118.
13 M. Li, X. Zhou, W. Ding, S. Guo and N. Wu, *Biosens. Bioelectron.*, 2013, **41**, 889–893.
14 Y. Xu, Z. Liu, X. Zhang, Y. Wang, J. Tian, Y. Huang, Y. Ma, X. Zhang and Y. A. Chen, *Adv. Mater.*, 2009, **21**, 1275–1279.
15 Y. Liu, R. Deng, Z. Wang and H. Liu, *J. Mater. Chem.*, 2012, **22**, 13619–13624.
16 A. Bianco, *Angew. Chem. Int. Ed.*, 2013, **52**, 4986–4997.
17 E. L. K. Chng and M. Pumera, *Chem. Eur. J.*, 2013, **19**, 8227–8235.
18 D. R. Dreyer, S. Park, C. W. Bielawski and R. S. Ruoff, *Chem. Soc. Rev.*, 2010, **39**, 228–240.

19 U. Hofmann and R. Holst, *Ber. Dtsch. Chem. Ges.*, 1939, **72**, 754–771.
20 G. Ruess, *Monatsch. Chem.*, 1946, **76**, 381–417.
21 W. Scholz, *Z. Anorg. Allg, Chem.*, 1969, **369**, 327–340.
22 T. Nakajima, and Y. Matsuo, *Carbon*, 1994, **32**, 469–475.
23 H. He, T. Riedl, A. Lerf, and J. Klinowski, *J. Phys. Chem*., 1996, **100**, 19954-19958.
24 H. He, J. Klinowski, M. Forster and A. Lerf, *Chem. Phys. Lett.*, 1998, **287**, 53–56.
25 A. Lerf, H. He, M. Forster, and J. Klinowski, *J. Phys. Chem. B*, 1998, **102**, 4477–4482.
26 T. Szabó, O. Berkesi, P. Forgó, K. Josepovits, Y. Sanakis, D. Petridis and I. Dékány, *Chem. Mater.*, 2006, **18**, 2740–2749.
27 W. Gao, L. B. Alemany, L. Ci and P. M. Ajayan, *Nat. Chem.,* 2009, **1**, 403–408.
28 A. M. Dimiev, L. B. Alemany and J. M. Tour, *ACS Nano,* 2013, **7**, 576–588.
29 L. Staudenmaier, *Ber. Dtsch. Chem. Ges.*, 1898, **31**, 1481–1487.
30 U. Hofmann and E. König, *Z. Anorg. Allg. Chem.*, 1937, **234**, 311–336.
31 W. S. Hummers and R. E. Offeman, *J. Am. Chem. Soc.*, 1958, **80**, 1339–1339.
32 D. C. Marcano, D. V. Kosynkin, J. M. Berlin, A. Sinitskii, Z. Sun, A. Slesarev, L. B. Alemany, W. Lu and J. M. Tour, *ACS Nano*, 2010, **4**, 4806–4814.
33 C. K. Chua, Z. Sofer, and M. Pumera, *Chem. Eur. J.,* 2012, **18**, 13453–13459.
34 A. Y. S. Eng, A. Ambrosi, C. K. Chua, F. Šaněk, Z. Sofer, and M. Pumera, *Chem. Eur. J.*, 2013, **19**, 12673–12683.
35 A. Y. S. Eng and M. Pumera, *Electrochem. Commun.*, 2014**, 43**, 87–90.
36 C. S. Lim, C. K. Chua, and M. Pumera, *J. Phys. Chem. C*, 2014, **118**, 23368−23375.
37 M. Pumera, *Electrochem. Commun.,* 2013, ***36***, 14–18.
38 S. You, S. M. Luzan, T. Szabó and A. V Talyzin, *Carbon*, 2013, **52**, 171–180.
39 P. D. Jannakoudakis, A. D. Jannakoudakis, E. Theodoridou and J. O. Besenhard, *J. Appl. Electrochem*., 1989, **19**, 341–344.
40 P. Chen, M. A. Fryling and R. L. McCreery, *Anal. Chem.*, 1995, **67**, 3115–3122.
41 P. Chen and R. L. McCreery, *Anal. Chem.*, 1996, **68**, 3958–3965.
42 M. M. Stylianakis, G. D. Spyropoulos, E. Stratakis and E. Kymakis, *Carbon*, 2012, **50**, 5554–5561.
43 C. A. Thorogood, G. G. Wildgoose, J. H. Jones and R. G. Compton, *New J. Chem.*, 2007, **31**, 958–965.
44 M. A. Fryling, J. Zhao and R. L. McCreery, *Anal. Chem.,* 1995, **67**, 967–975.
45 C. A. Thorogood, G. G. Wildgoose, A. Crossley, R. M. J. Jacobs, J. H. Jones and R. G. Compton, *Chem. Mater.*, 2007, **19**, 4964–4974.
46 G. G. Wildgoose, P. Abiman and R. G. Compton, *J. Mater. Chem.*, 2009, **19**, 4875–4886.
47 A. T. Masheter, L. Xiao, G. G. Wildgoose, A. Crossley, J. H. Jones and R. G. Compton, *J. Mater. Chem.*, 2007, **17**, 3515–3524.
48 R. S. Sundaram, *Chemically Derived Graphene* In *Graphene: Properties, Preparation, Characterisation and Devices*, ed. V. Skakalova and A. B. Kaiser, Woodhead Publishing UK, 2014, pp 50–80.
49 N. A. Kumar, H.-J. Choi, Y. R. Shin, D. W. Chang, L. Dai and J.-B. Baek, *ACS Nano*, 2012, **6**, 1715–1723.
50 E. L. K. Chng and M. Pumera, *Chem. Asian J.*, 2011, **6**, 2899–2901.
51 J. G. S. Moo, A. Ambrosi, A. Bonanni and M. Pumera, *Chem. Asian J.*, 2012, **7**, 759–770.
52 A. Bonanni, A. Ambrosi and M. Pumera, *Chem. Eur. J.*, 2012, **18**, 4541–4548.
53 A. Hunt, D. A. Dikin, E. Z. Kurmaev, T. D. Boyko, P. Bazylewski, G. S. Chang and A. Moewes, *Adv. Funct. Mater.*, 2012, **22**, 3950–3957.
54 K. Erickson, R. Erni, Z. Lee, N. Alem, W. Gannett and A. Zettl, *Adv. Mater.*, 2010, **22**, 4467–4472.
55 W. H. Lee, S. J. Kim, W. J. Lee, J. G. Lee, R. C. Haddon and P. J. Reucroft, *Appl. Surf. Sci.*, 2001, **181**, 121–127.
56 E. Bekyarova, M. E. Itkis, P. Ramesh, C. Berger, M. Sprinkle, W. A. de Heer and R. C. Haddon, *J. Am. Chem. Soc.*, 2009, **131**, 1336–1337.
57 Y. Feng, H. Liu, W. Luo, E. Liu, N. Zhao, K. Yoshino and W. Feng, *Sci. Rep.*, 2013, **3**, 3260.
58 J. Coates, *Interpretation of Infrared Spectra, A Practical Approach.* In *Encylopedia of Analytical Chemistry*, ed. R. A. Meyers, Wiley UK, 2000, pp 10815–10837.
59 W. Cai, R. D. Piner, F. J. Stadermann, S. Park, M. A. Shaibat, Y. Ishii, D. Yang, A. Velamakanni, S. J. An, M. Stoller, J. An, D. Chen and R. S. Ruoff, *Science*, 2008, **321**, 1815–1817.
60 A. B. Bourlinos, D. Gournis, D. Petridis, T. Szabó, A. Szeri and I. Dékány, *Langmuir*, 2003, **19**, 6050–6055.
61 S. Wang, P.-J. Chia, L.-L. Chua, L.-H. Zhao, R.-Q. Png, S. Sivaramakrishnan, M. Zhou, R. G.-S. Goh, R. H. Friend, A. T.-S. Wee and P. K.-H. Ho, *Adv. Mater.*, 2008, **20**, 3440–3446.
62 H. Yang, C. Shan, F. Li, D. Han, Q. Zhang and L. Niu, *Chem. Commun.*, 2009, 3880–3882.
63 M. Banerjee, A. Gupta, S. K. Saha and D. Chakravorty, *Small*, 2015, DOI: 10.1002/smll.201500200.
64 G. I. Titelman, V. Gelman, S. Bron, R. L. Khalfin, Y. Cohen and H. Bianco-Peled, *Carbon*, 2005, **43**, 641–649.
65 R. Yuge, M. Zhang, M. Tomonari, T. Yoshitake, S. Iijima and M. Yudasaka, *ACS Nano,* 2008, **2**, 1865–1870.
66 S. Niyogi, E. Bekyarova, M. E. Itkis, J. L. McWilliams, M. A. Hamon and R. C. Haddon, *J. Am. Chem. Soc.*, 2006, **128**, 7720–7721.
67 J. S. Park, S. M. Cho, W.-J. Kim, J. Park and P. J. Yoo, *ACS Appl. Mater. Interfaces*, 2011, **3**, 360–368.

Table of Contents text

The various oxygen functional groups in graphite oxide are investigated by synthetic labelling and an electrochemical detection approach.

This journal is © The Royal Society of Chemistry 20xx